

Numerical study of Holstein's molecular-crystal model: Adiabatic limit and influence of phonon dispersion

Hans De Raedt

Physics Department, University of Antwerp, Universiteitsplein 1, B-2610 Wilrijk, Belgium

Ad Lagendijk

Natuurkundig Laboratorium, University of Amsterdam, Valckenierstraat 65, 1018-XE Amsterdam, The Netherlands

(Received 28 February 1983; revised manuscript received 14 September 1983)

We report on simulations for the molecular-crystal model without dispersion in the adiabatic regime for all lattice dimensionalities. A discrete version of the Feynman path-integral formalism is used to calculate the electron properties. We compare these results with approximate theories and conclude that continuum versions of the molecular-crystal model have little relationship to the discrete lattice model. In addition, the influence of the phonon dispersion on the transition between the "untrapped" and "self-trapped" state of an electron on a one-dimensional lattice is studied within the context of Holstein's molecular-crystal model. We show that the electron-phonon interaction has a critical value below which self-trapping does not occur. We find that this critical value goes to zero if the optical phonon becomes soft.

I. INTRODUCTION

In a previous study,¹ hereafter referred to as I, we have shown that the thermodynamics and ground-state properties of the molecular-crystal model² (MCM) can be sampled very accurately by path-integral Monte Carlo techniques. Monte Carlo results are rigorous measurements of finite-size systems and if the size effects are small [as is the case for the MCM (Ref. 1)] they represent the behavior of the infinite-size system. Monte Carlo results can be used to test the validity of approximate variational or adiabatic theories.

Holstein's molecular-crystal model² consists of an electron described by a tight-binding Hamiltonian interacting with harmonic lattice vibrations through a short-range potential. This lattice polaron is expected to exhibit fascinating properties of which the most important for us is the possible nonanalytic behavior of thermodynamic observables as a function of the coupling constant.³⁻⁵ In I we discussed our results for the one-dimensional (1D), 2D, and 3D MCM's in the case of dispersionless phonons. In this paper we originally intended to report results on the 1D model with phonon dispersion. However, reactions to the content of I have led us to discuss in addition and in more detail the relation between our results, including those of I, and various approximate theories. As a consequence, we will also report on our recently obtained simulation results for parameters which are much closer to the adiabatic regime than those used in I.

II. DISPERSIONLESS MODEL

For simplicity of notation we will now formulate the theory in one space dimension. The formulas for 2D and 3D systems can be derived by means of the same technique but we will not present them here. The model Hamiltonian reads

$$H = H_0 + H_1 + H_2, \quad (2.1a)$$

$$H_0 = \frac{1}{2m_0} \sum_{i=1}^M p_i^2, \quad (2.1b)$$

$$H_1 = \frac{m_0 \Omega^2}{2} \sum_{i=1}^M x_i^2 + \lambda \sum_{i=1}^M x_i c_i^\dagger c_i, \quad (2.1c)$$

$$H_2 = -t \sum_{i=1}^M c_i^\dagger c_{i+1} + c_{i+1}^\dagger c_i. \quad (2.1d)$$

Ω is the angular frequency of the Einstein oscillator, λ is the fermion-boson coupling strength and t is the kinetic energy associated with the nearest-neighbor hopping motion of the fermion. The momentum and coordinate of the i th boson are denoted by p_i and x_i , c_i^\dagger creates a fermion at site i , and c_i removes a fermion from site i .

Hamiltonian (2.1) describes an electron coupled linearly to the phonon field of the site where the electron resides. The phonons are dispersionless and consequently the only intersite communication is through the electron. Physical realizations of the d -dimensional model could be found in molecular crystals. One needs a molecular unit compatible with the lattice symmetry and having a nondegenerate internal mode, for instance, the breathing mode.

In principle, four parameters enter Hamiltonian (2.2): t , the force constant of the Einstein oscillator, κ , the mass of the Einstein oscillator, m_0 , and the electron-phonon coupling λ . However, the theory can be presented using only three independent (energy) parameters: t , λ^2/κ , and $(\kappa/m_0)^{1/2}$ or equivalently t , $\lambda^2/m_0\Omega^2$, and Ω . Usually we will set our energy scale by setting $\Omega=1$, but in the adiabatic limit ($m_0 \rightarrow \infty$, κ finite) this is not so elegant and we will retain Ω . Several limits can be distinguished: (i) the weak-coupling limit ($\lambda^2/m_0\Omega^2 \ll t, \Omega$), (ii) the adiabatic limit, (iii) the strong-coupling limit ($\lambda^2/m_0\Omega^2 \gg t, \Omega$), and (iv) the small- t limit ($t \ll \lambda^2/m_0\Omega^2, \Omega$). A rigorous analytic adiabatic solution for the MCM on a lattice does not

seem to have been found yet. Several adiabatic solutions for a continuum version of the model have been given.^{2,4-6} Holstein has treated the small- t limit.² The weak-coupling limit can be treated with standard perturbation theory.^{7,8} The strong-coupling regime is part of the adiabatic regime.

Our simulations of the MCM as reported in I were done for the extreme quantum limit, $t \approx \Omega$. This regime is outside the range of validity of any perturbation theory and poses the most severe tests for the Monte Carlo algorithm. To approach the adiabatic domain we have now performed simulations with $t=1$ and Ω down to 0.01. Before discussing these simulation results we will outline some of the features of the small polaron as emerging from previous approximate analytic theories and our own Monte Carlo study.

Emin has introduced a variational wave function which is a good starting point to establish the physics of the small polaron.⁵ His wave function can be represented as

$$\psi_{\vec{k}} = N^{-1/2} \sum_{\vec{q}} e^{i\vec{k} \cdot \vec{q}} c_{\vec{q}}^{\dagger} \prod_{\vec{q}} \exp[f_{\vec{q}}(\vec{k}) e^{i\vec{q} \cdot \vec{q}} b_{\vec{q}} - f_{\vec{q}}^*(\vec{k}) e^{-i\vec{q} \cdot \vec{q}} b_{\vec{q}}^{\dagger}] |0\rangle, \quad (2.2)$$

in which $b_{\vec{q}}$ is the destruction operator of vibrational mode \vec{q} and N is the number of sites. In (2.2) the $f_{\vec{q}}(\vec{k})$ are (complex) variational parameters. Several possible choices for this set of variational parameters are of interest. If all $f_{\vec{q}}(\vec{k})=0$ the wave function refers to an undistorted lattice. If $f_{\vec{q}}(\vec{k})$ is nonzero for $|\vec{q}| < q_0$ the polaron is characterized by a local distortion. The polaron has an exponentially decaying amplitude in real space, the characteristic size being proportional to q_0^{-1} . If $f_{\vec{q}}(\vec{k}) = \text{const} \neq 0$ the local distortion is restricted to a single site. It is this situation which is usually called the small polaron's self-trapped state.

In this homogeneous model there is no possibility for breaking the translational symmetry. Wave function (2.2) is manifestly translational invariant. So if one talks about a phase transition in the ground state of the MCM one refers to the change in the local "building block" of the Bloch wave function. Of course, time scales for tunneling might become very long but this is not a critical effect. Any small symmetry-breaking field will cause absolute localization to occur. In nature these fields may be due to small crystal inhomogeneities which are always present in a real crystal. In this respect the problem is quite analogous to the dynamic Jahn-Teller effect. Without disorder the Jahn-Teller effect is always dynamic and does not involve any symmetry breaking.⁹

In our work the small polaron is treated with path-integral techniques and the problem is solved without using wave functions. This is certainly not a disadvantage because only observables are of interest. In the path-summation approach these observables are obtained directly. An observable that we found very suitable to characterize the polaron is $\hat{C}(l) = \sum_i \langle c_i^{\dagger} c_{i+l} \rangle$, because

it measures the extent of the polaron. In the self-trapped state one expects $\hat{C}(l) = \hat{C}(0)\delta_{l,0}$. The best way to study this correlation function is to follow it as a function of l at each λ and to try to fit to it various simple functions such as an exponential. It is instructive to evaluate $\hat{C}(l)$ in the weak-coupling limit. In one dimension the result is

$$\hat{C}(l) = \lambda(2m_0\Omega)^{-1/2} M^{-1} \sum_k \frac{\cos(kl)}{\Omega + 2t - 2t \cos k}, \quad (2.3a)$$

$$= \lambda[2m_0\Omega^2(\Omega + 4t)]^{-1/2} \left[\frac{\Omega + 2t - (\Omega^2 + 4t\Omega)^{1/2}}{2t} \right]^{|l|}. \quad (2.3b)$$

Equation (2.3a) is readily generalized to higher dimensions in terms of the lattice Green function, the results for all dimensions being an exponential decay of $\hat{C}(\vec{l})$.¹⁰ Equation (2.3b) implies a correlation length of

$$-1/\ln\{[\Omega + 2t - (\Omega^2 + 4t\Omega)^{1/2}/2t]\}.$$

Furthermore,

$$\sum_{\vec{l}} \hat{C}(\vec{l}) = N \langle x_{\vec{l}} \rangle, \quad (2.4)$$

which in the weak-coupling limit is equal to $\lambda\Omega^{-3/2}(2m_0)^{-1/2}$ for any dimension. From (2.3) we see that in the weak-coupling regime decreasing Ω or increasing t will increase the size of the polaron. There is also a remarkable relationship between $\hat{C}(\vec{l})$ and the variational parameters $f_{\vec{q}}(\vec{k})$ that enter Emin's trial wave function (2.2). If we use (2.2) to approximate $\hat{C}(\vec{l})$ we find that it is directly related to the spatial Fourier transform of $f_{\vec{q}}(\vec{k})$.

It is very computer-time consuming to monitor $\hat{C}(\vec{l})$ for many \vec{l} values. Since we are investigating the self-trapped states of the polaron it is sufficient to study $\hat{C}(\vec{l})$ for a few, small $|\vec{l}|$ values. Self-trapping will show up as a vanishing of all $\hat{C}(\vec{l})$ except $\hat{C}(0)$. It was exactly this correlation function which was sampled in I and gave strong evidence for self-trapping in one, two, and three dimensions. In I we have also sampled the kinetic energy as a function of the coupling and we observed that an increase of the coupling resulted in a smooth gradual decrease of the kinetic energy. In the regime where self-trapping occurs the kinetic energy does not vanish and we have taken this smooth behavior as indication that no effects of translational-symmetry breaking are present.

If a model is expected to show nonanalytic behavior in some of its thermodynamic functions or in its ground-state properties one would like to know the character of these nonanalyticities. One can think of first-order-type behavior with coexistence of different phases or of second-order-type behavior with critical fluctuations or of even different (e.g., higher-order) transitions. In such a case one investigates the susceptibilities of the driving fields. Since the electron-phonon coupling is the driving force in the occurrence of self-trapping, it is obvious that one should focus on the derivatives of the polaron free energy F^E with respect to the coupling parameter. If there

are no peculiarities in these quantities there is no transition. The first derivative of the polaron free energy $\partial F^E/\partial\lambda$ is equal to the coupling energy and $\partial^2 F^E/\partial\lambda^2$ is related to the coupling-energy—coupling-energy static susceptibility. In I it was shown that $\partial^2 F^E/\partial\lambda^2$ exhibits a sharp maximum as a function of λ . One contribution to $\partial^2 F^E/\partial\lambda^2$ is proportional to $\partial F^E/\partial\lambda$ and subtracting this background yields the susceptibility χ . This thermodynamic function could be sampled directly during the simulations and, as reported in I, gave evidence for strong fluctuations in the system when λ approaches its critical value. Both the observation of enhanced fluctuations and the sharp drop in $\hat{C}(\vec{l})/\hat{C}(0)$ for $|\vec{l}|=1$ were interpreted by us as evidence for a continuous transition with a possible divergence of a higher-order derivative of the free energy. The observed critical value of the coupling constant could be estimated rather accurately by equating strong- and weak-coupling expressions for the ground-state energy. All these results were obtained from simulations at very low temperature and relate to ground-state properties. Elevating the temperature immediately wipes out all critical effects. Qualitatively, we found no dependence on dimensionality: That is to say, for all lattice dimensionalities we observed enhanced fluctuations and self-trapping effects at finite values of the coupling constant. We did find quantitative differences which we could not yet exploit due to the lack of theories that describe the self-trapping process qualitatively correctly.

An approach directly addressing the presence of a phase transition in the lattice model without invoking the adiabatic approximation is the variational calculation for the 3D model of Emin.⁵ Emin finds that two types of polarons, the self-trapped carrier and the untrapped (band) carrier, coexist for a range of values of the coupling constant. His discontinuous transition becomes continuous only at very small bandwidths ($6t/\Omega \approx 1$). It is well known that the rigidity of a variational calculation can easily induce artifacts in critical behavior. As noted by Sumi and Toyozawa³ two coexisting solutions of a variational calculation which are not orthogonal should be combined in two orthogonal linear combinations. In this way discontinuous behavior disappears. Our results are in conflict with Emin's variational calculation. More elaborate approximations also rule out the occurrence of a first-order phase transition.¹¹

A rigorous adiabatic solution does not seem to have been reported for the lattice model. Appel⁶ reviews some work on the basis of which he concludes that in one dimension the character of the ground state will change when $4t \approx \lambda^2/m_0\Omega^2$. This would not be in conflict with our work. Our empirical formula,

$$\lambda^2 = 4tm_0\Omega^2[1 - \Omega(4t\Omega + \Omega^2)^{-1/2}]^{-1}, \quad (2.5)$$

reduces to Appels's estimate in the adiabatic region. One must also be very careful in using zeroth-order adiabatic Born-Oppenheimer wave functions for the MCM because they manifestly break translational invariance.

Much work has been done on continuum approximations to the MCM. Only the 1D version of these is well behaved and cutoff free. Emin and Holstein interpret their results as follows: in one dimension there is ex-

ponential localization (no zero-size self-trapping), in two dimensions the polaron is either unbound (infinite size) or self-trapped (zero size), and in three dimensions unbound and self-trapped states are both stable and coexist.^{4,5} Our previous work as reported in I referred to the $t \approx \Omega$ domain of the model parameter space and is certainly in disagreement with the interpretation of adiabatic studies of the continuum model. This discrepancy could be caused by the nonadiabatic corrections or by the discreteness of the model. Therefore we performed simulations for $t=1$ and decreasing Ω , down to $\Omega=0.01$ for both 1D and 3D systems. The technical details with respect to extensive convergence tests and comparisons, wherever possible, with results from perturbation theory and from asymptotic analysis, will be given in a later section when we discuss Monte Carlo results of the MCM with phonon dispersion. We do not display the results because apart from a trivial change in scale (in I, Ω and m_0 were set equal to 1) they are very similar to the results reported in I. This means that the discrepancy between I and adiabatic studies of the continuum version of the MCM is due to the continuum approximation. As a matter of fact, Emin and Holstein already pointed out an essential difference between continuum and lattice descriptions: In the lattice model the kinetic energy is bounded from above, whereas in the continuum version it is not. Therefore localization is always more difficult in the continuum model. This would explain the absence of zero-size self-trapping in the 1D continuum model. When discussing self-trapping in one dimension one should realize that no translational-symmetry breaking is involved in self-trapping. For this reason the common wisdom "in one dimension everything is localized" is not relevant for the present homogeneous polaron model. There is no discrepancy in two dimensions because an unbound polaron in a continuum will very likely become a band polaron in a discrete lattice. At least this is true for the weak-coupling limit in any dimension [see Eq. (2.3a)]. In three dimensions the coexistence of the self-trapped and unbound band states in the continuum model is in disagreement with our simulation data of the lattice MCM. It is obvious that quantum fluctuations of lattice vibrations, neglected in the adiabatic approximation, might strongly influence the possible coexistence of the two states. However, since we did not find any significant dependence of the critical behavior on Ω (down to $\Omega=0.01$), we believe that the coexistence found in the continuum adiabatic theory is mainly caused by the use of the continuum approximation. It should be realized that the region in parameter space where one expects the continuum approximation to work well, i.e., when the polaron is much larger than the lattice spacing, is different from the region where the phenomenon of self-trapping is occurring.

The MCM is also expected to exhibit some interesting transport properties at nonzero temperature. In principle, our path-summation method gives information on static properties only and no results on dynamical correlation functions. However, transport anomalies often arise from critical or otherwise peculiar behavior of static quantities such as static susceptibilities. On the basis of this we can add some comments on transport properties. Tempera-

ture has dramatic effects on bound states, a simple example being the hydrogen atom which is a bound object at zero temperature only. With this in mind we are not surprised to find that the main effect of nonzero temperature is to diminish and smear out critical effects. It is, of course, still possible that the MCM displays temperature-dependent transport anomalies, but it is very likely that they are not related to interesting behavior of static quantities. Emin uses his variational calculation to construct a model with transport anomalies due to a "temperature-dependent" energy spectrum.⁵ It would be very interesting if new variational work in the spirit of Emin's calculation could be done such that there would be better agreement with our computer experiments.

III. 1D MODEL WITH PHONON DISPERSION

A. Technicalities

The modified MCM is written as

$$H = H_0 + H_1 + H_2, \quad (3.1a)$$

$$H_0 = \frac{1}{2m_0} \sum_{i=1}^M p_i^2, \quad (3.1b)$$

$$H_1 = \frac{m_0 \omega_0^2}{2} \sum_{i=1}^M x_i^2 + \frac{m_0 \omega_1^2}{2} \sum_{i=1}^M x_i x_{i+1} + \lambda \sum_{i=1}^M x_i c_i^\dagger c_i, \quad (3.1c)$$

$$H_2 = -t \sum_{i=1}^M (c_i^\dagger c_{i+1} + c_{i+1}^\dagger c_i). \quad (3.1d)$$

The phonon dispersion has been introduced by allowing for nearest-neighbor coupling of the oscillators. Note that

$$\Omega(q) \equiv \left[\omega_0^2 + \omega_1^2 \cos \left(\frac{2\pi q}{M} \right) \right]^{1/2}$$

is the frequency of a vibration with wave vector $2\pi q/M$ (the lattice spacing is 1).

We now proceed as in the case of dispersionless phonons¹ where we used the Trotter formula¹² to derive a path-integral representation of the partition function. We have

$$Z \equiv \text{Tr} e^{-\beta H} = \lim_{m \rightarrow \infty} Z_m, \quad (3.2a)$$

$$Z_m = \text{Tr} \left[\exp \left(\frac{-\beta H_0}{m} \right) \exp \left(\frac{-\beta H_1}{m} \right) \right. \\ \left. \times \exp \left(\frac{-\beta H_2}{m} \right) \right]^m. \quad (3.2b)$$

To calculate the trace in (3.2b) we evaluate the matrix elements of each product in (3.2b) using the coordinate representation of the phonon-field and occupation-number representation of the fermion. Hamiltonian (3.1) is quadratic in the phonon coordinates and therefore we can carry out the integrals over the phonon coordinates analytically. The final results read

$$Z_m = c Z_m^P Z_m^E, \quad (3.3a)$$

$$Z_m^P = \prod_{q=1}^M \prod_{k=1}^m a_k^{-1/2}(q), \quad (3.3b)$$

$$Z_m^E = \sum_{\{y_l\}} \rho(\{y_l\}), \quad (3.3c)$$

$$\rho(\{y_l\}) = \left[\prod_{j=1}^m I \left[\frac{2\beta t}{m}, y_j - y_{j+1} \right] \right] \\ \times \exp \left[\sum_{i=1}^m \sum_{j=1}^m F(i-j, y_i - y_j) \right], \quad (3.3d)$$

$$F(l, y) = \frac{\beta^3 \lambda^2}{4m_0 m^4 M} \sum_{q=1}^M \sum_{k=1}^m a_k^{-1}(q) \cos \left[\frac{2\pi k l}{m} \right] \\ \times \cos \left[\frac{2\pi q y}{M} \right], \quad (3.3e)$$

$$I(z, l) = \frac{1}{M} \sum_{n=1}^M \cos \left[\frac{2\pi l n}{M} \right] \exp \left[z \cos \left[\frac{2\pi n}{M} \right] \right], \quad (3.3f)$$

$$a_k(q) = 1 - \cos \left[\frac{2\pi k}{m} \right] + \frac{1}{2} \left[\frac{\beta \Omega(q)}{m} \right]^2. \quad (3.3g)$$

All unimportant numerical factors have been absorbed in the constant C in Eq. (3.3a). Taking the adiabatic limit has an effect on the function $F(l, y)$ only. In the adiabatic limit [i.e., neglecting the kinetic energy of the phonons in (3.2)], $F(l, y)$ becomes

$$F(l, y) = \frac{\beta \lambda^2}{2m_0 m^2 M} \sum_{q=1}^M \Omega^{-2}(q) \cos \left[\frac{2\pi q y}{M} \right], \quad (3.3h)$$

which reduces to

$$F(l, y) = \frac{\beta \lambda^2}{2m_0 \omega_0^2 m^2} \delta_{y,0} \quad (3.3i)$$

if there is no phonon dispersion. Note that in the adiabatic limit $F(l, y)$ leads to infinite-range interactions in the Trotter direction.

For computational purposes it is convenient to express the oscillation frequencies in terms of the gap g of the phonon frequency at the Brillouin-zone boundary. Thereby we fix the energy scale such that $\Omega(q=0) = 1$ and obtain

$$\omega_0^2 = \frac{1+g^2}{2}, \quad \omega_1^2 = \frac{1-g^2}{2}. \quad (3.4)$$

The approximation Z_m^P to the partition function of the free-phonon system can be calculated to any desired precision. The calculation of the electron contribution Z_m^E is not trivial because it describes a peculiar two-dimensional system of m mutually interacting particles at the positions y_j . The first factor in (3.3d) represents the effective nearest-neighbor interaction due to the hopping motion, and the second accounts for the retarded long-range interactions caused by the electron-phonon coupling. Note that the m particles can only move such that each of the m replicas of the one-dimensional quantum system contains exactly one particle.

Formally, the results (3.3) are equivalent to Feynman's

result for the Fröhlich polaron,¹³ the index j playing the role of the imaginary time that appears in the path integral. Obviously, (3.3) reproduces the exact zero- and infinite-coupling results for any value of m . It can be shown¹⁴ that $Z_m \geq Z_{m+1} \geq Z$ and consequently we will obtain lower bounds on the free energy instead of the upper bounds obtained by conventional variational methods.

Although in a strict sense the density function in (3.3) is not a density function of a genuine 2D classical model, we can still use the Metropolis Monte Carlo technique¹⁵ to calculate estimators of the thermal expectation values. By doing so we avoid approximations such as perturbation expansions or variational procedures. The analytic elimination of the phonon degrees of freedom enables us to study the polaron properties quantitatively because the problem has been reformulated such that the polaron contribution can be calculated separately. When not only the fermion but also the boson properties are calculated simultaneously by a Monte Carlo technique, the polaron contribution is hidden in the statistical noise of the phonons because there are mM phonon variables, whereas there are only m electron degrees of freedom. The most important advantage of our approach is that it combines analytic and numerical techniques in such a way that the simulation itself is very efficient.

The thermodynamic functions of interest are the approximations to the energy and derivatives of the free energy $F_m^E = -(1/\beta)\ln(Z_m^E)$ with respect to the coupling λ . The first derivative of the free energy is related to the expectation value of the electron-phonon interaction $\sum_i x_i c_i^\dagger c_i$. The fluctuation of this quantity is given by the static (Kubo) susceptibility

$$\chi_m = -\frac{\partial^2 F_m^E}{\partial \lambda^2} - \frac{1}{\lambda} \frac{\partial F_m^E}{\partial \lambda}. \quad (3.5a)$$

Analytic evaluation of the derivatives gives

$$\begin{aligned} \chi_m = & \frac{4}{\beta \lambda^2} \sum_{i=1}^m \sum_{j=1}^m \sum_{i'=1}^m \sum_{j'=1}^m \langle F(i-j, y_i - y_j) \\ & \times F(i'-j', y_{i'} - y_{j'}) \rangle \\ & - \frac{4}{\beta \lambda^2} \left[\sum_{i=1}^m \sum_{j=1}^m \langle F(i-j, y_i - y_j) \rangle \right]^2. \end{aligned} \quad (3.5b)$$

Here and in the following formulas, $\langle A \rangle$ denotes the expectation value with respect to the density function $\rho(\{y_i\})$ given by (3.3d). A discontinuity in $\partial F_m^E / \partial \lambda$ or χ_m as a function of λ implies that the free energy is not an analytic function of the coupling λ . If there exists a critical coupling λ_c for the electron-lattice interaction for which F_m^E or one of its derivatives with respect to λ is singular, the system undergoes a transition from one (ground) state to another.

It is well known¹⁵ that it is difficult to estimate the free energy by means of the Metropolis Monte Carlo technique. However, we can use the Monte Carlo technique to sample the expectation values of the correlation functions that appear in the expressions for the derivatives of F_m^E . In this way we also avoid the ambiguities that arise when

the derivatives of the free energy are obtained by numerical differentiation.

In order to gain additional insight in the phenomenon of self-trapping we also calculate the electron-phonon correlation functions

$$\hat{C}(l) = \sum_{i=1}^M \frac{\text{Tr} e^{-\beta H} c_i^\dagger c_i x_{i+l}}{\text{Tr} e^{-\beta H}}. \quad (3.6a)$$

Analytic elimination of the phonons yields

$$\hat{C}(l) = \lim_{m \rightarrow \infty} \hat{C}_m(l), \quad (3.6b)$$

$$\hat{C}_m(l) \equiv \sum_{i,j=1}^m \langle F(i-j, y_i - y_j) \rangle. \quad (3.6c)$$

As mentioned in the preceding section, to interpret the simulation results of correlation functions (3.6c) we have found it expedient to introduce the normalized correlation functions

$$C_m(l) \equiv \hat{C}_m(l) / \hat{C}_m(0). \quad (3.7)$$

The size of the polaron can be extracted from the l dependence of correlation functions (3.7).

B. Discussion

It should be clear that keeping m finite is the only approximation that has been made so far and therefore it is necessary to study the convergence of the results as a function of m . The very essence of our approach is to compute the relevant physical properties as a function of the number of imaginary-time slices m . According to the Trotter formula¹² the results of such a calculation should converge to the exact results if $m \rightarrow \infty$. The convergence of the phonon contribution Z_m^P can be studied numerically without much difficulty but since we are unable to evaluate (3.3c) analytically, we have to employ a simulation technique to calculate the polaron path integral. We calculate the thermal expectation value of the observables by simulating a system of m particles on a computer and therefore it is important to know the minimum value of β/m for which the difference between exact and approximate results is small.

As the present work is mainly concerned with determining the effect of the phonon dispersion on the existence of the untrapped-self-trapped transition, it is necessary to perform simulations at sufficiently low temperature. For the range of phonon frequencies chosen in the preceding subsection [see (3.4)] and transfer energy $t=1$, an inverse temperature $\beta=5$ already corresponds to a low temperature for the system under consideration. In the presence of phonon dispersion, the vibrational state of the system depends not only on the temperature but also on the gap g of the phonon frequency at the Brillouin-zone boundary. If $\beta g \ll 1$ there will be a large number of phonons of wave vector close to π , but because the frequency of these vibrations is small we might expect that a description at a more classical level ($m \rightarrow 1$) should be sufficient. In other words, for fixed β and m the approximation (3.4) becomes more accurate if the phonon gap g decreases. In I we showed that if the maximum phonon

frequency $\Omega(q=0)=1$, it is sufficient to take $m > 20$ in order to reproduce the exact results of the phonon energy with an error of less than 1%.

To study the convergence of the results as a function of m we have calculated the thermodynamic functions of the polaron as a function of m for a limited number of g values. The values of m used in the final simulations are taken such that the systematic errors resulting from the Trotter formula are hidden in the statistical noise of the simulation data. To determine the statistical errors due to the Monte Carlo procedure we have made several statistically independent runs for each set of parameters. In concert with our findings for the dispersionless model¹ we concluded that $m=32$ is a reasonable compromise between accuracy of the approximation (3.3) and the CPU times (CPU denotes central processing unit) required to simulate the model. Thus we will now concentrate on the data obtained from simulations for $\beta=5$, $t=1$, $\Omega(q=0)=1$, and $m=32$. In our final simulations, we chose $M=32$ (within the statistical errors the results for $M=64$ are the same) and 2000 m single-particle steps were discarded before taking 20 000 samples. The number of single-particle steps between two successive samples is m .

An important check on the results is the comparison with various analytic treatments in the appropriate limits. In the weak-coupling regime the thermal energy and the electron-phonon correlation functions [$\hat{C}(l)$] were compared with the results of second-order perturbation theory. In the strong-coupling regime the results were compared with Eqs. (3.9) and (3.11). In addition, some analytic results are known for the two-site polaron. In all these cases excellent agreement was obtained between the Monte Carlo results and the various approximations in the appropriate limits. The reader can get an impression of the agreement which was obtained by inspecting Fig. 3 of this paper and by inspecting Figs. 2, 5, and 7 of I.

As we have demonstrated in I the most direct indication for a transition is found by calculating the coupling-energy susceptibility χ_m as a function of λ . In Fig. 1 we show some typical results for χ_m for two values of the phonon gap g . These data strongly suggest that χ_m is discontinuous at the critical point $\lambda_c(g)$, but it is also obvious that it is impossible to prove this by means of Monte Carlo data. This problem of interpreting simulation data of a system at its critical point is very similar to the one encountered in Monte Carlo work on classical many-body systems.¹⁵ From Fig. 1 we already note that $\lambda_c(g)$ decreases with g . To investigate the g dependence of $\lambda_c(g)$ in more detail we have performed simulations for a large set of λ and g values. In Fig. 2 we depict the location of the maximum of χ_m as a function of g . In the case of dispersionless vibrations we already observed that a good empirical estimate of the critical coupling $\lambda_c(g=1)$ can be obtained by equating the weak- and strong-coupling expansion of the ground-state energy.¹ For the model (3.1) the weak-coupling result for the ground-state energy reads

$$E_{\text{weak}} = -2t - \frac{\lambda^2}{2m_0M} \sum_{q=1}^M G(q), \quad (3.8a)$$

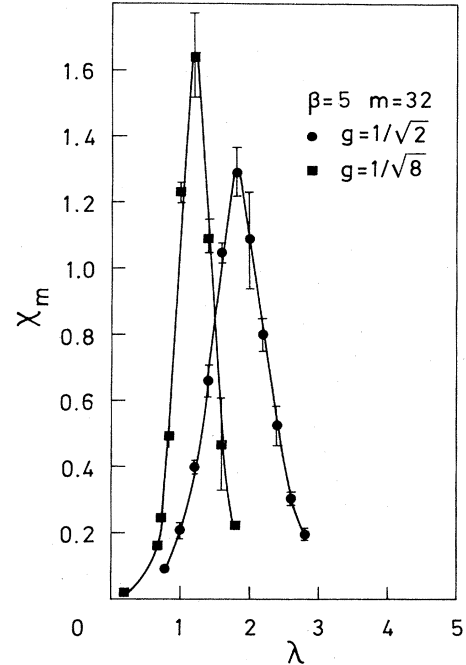


FIG. 1. Electron-phonon-coupling-energy susceptibility χ_m as a function of the electron-phonon coupling λ .

where

$$G(l) \equiv \Omega^{-1}(q) \left[2t - 2t \cos \left(\frac{2\pi q}{M} \right) + \Omega(q) \right]^{-1}. \quad (3.8b)$$

The strong-coupling limit is easily obtained from the path integral (3.3c) by observing that $\lim_{z \rightarrow 0} I(z, l) = \delta_{l,0}$ and it is then trivial to obtain

$$E_{\text{strong}} = -\frac{\lambda^2}{2m_0g}. \quad (3.9)$$

Note that the strong-coupling expression (3.9) can also be found by taking the small- t limit of (3.3). Solving the empirical equation $E_{\text{weak}} = E_{\text{strong}}$ for different g yields

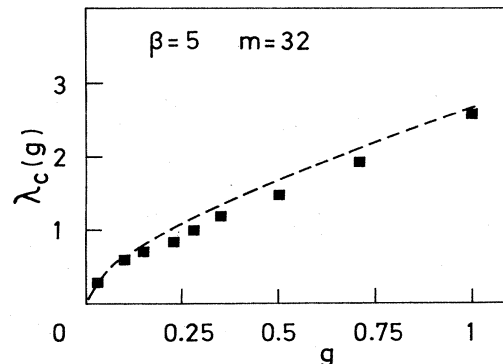


FIG. 2. Critical value $\lambda_m(g)$ of the electron-phonon coupling as a function of the phonon gap g at the Brillouin-zone boundary. The dashed line is a theoretical result obtained from comparison of weak- and strong-coupling expansions.

$$\lambda_c(g) = 2(gtm_0)^{1/2} \left[1 - \frac{g}{M} \sum_{q=1}^M G(q) \right]^{-1/2}. \quad (3.10)$$

This gives a good estimate of the critical coupling $\lambda_c(g)$. The dashed line in Fig. 2 is the result of a straightforward numerical evaluation of (3.10). It is clear that the estimates obtained from the simulation data are in good agreement with the theoretical prediction. Assuming that (3.10) will still hold if $g \rightarrow 0$ (the smallest phonon gap used in our simulations is $g=0.03$) it is not difficult to show that $\lim_{g \rightarrow 0} \lambda_c(g) = 0$. Thus the electron will always be in the self-trapped state if the phonons become soft.

In Fig. 3 we have plotted the normalized electron-phonon correlation function (3.8). To interpret the data it is expedient to consider the limits of weak and strong electron-phonon interactions. We find

$$\lim_{T \rightarrow 0} \lim_{\lambda \rightarrow 0} C(l) = \left[\sum_{q=1}^M G(q) \cos \left[\frac{2\pi l q}{M} \right] \right] / \sum_{q=1}^M G(q), \quad (3.11a)$$

$$\lim_{\lambda \rightarrow \infty} C(l) = \left[\frac{g-1}{g+1} \right]^l. \quad (3.11b)$$

From Fig. 3 we conclude that the simulation data for weak and strong coupling are in excellent agreement with the weak- and strong-coupling expansions. Moreover, it yields reliable results for the intermediate-coupling regime, a regime which is not amenable to the conventional expansion techniques. In this intermediate-coupling regime the transition between weak- and strong-coupling behavior is signaled by the rapid change of $C(l)$. From our discussion of the g dependence of the critical coupling

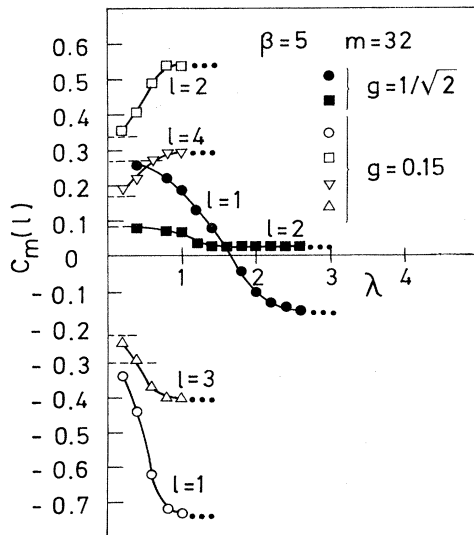


FIG. 3. Normalized electron-phonon correlation functions $C(l)$ for two values of the phonon gap g as a function of the distance l and the electron-phonon coupling λ . The dashed lines are the results of a weak-coupling theory; the values obtained from the strong-coupling theory are represented by three (small) dots. Solid lines are guides for the eye only.

constant one could have expected that the region of validity of the weak-coupling theory vanishes as g approaches zero and Fig. 3 shows that this is indeed the case. The phonon frequency has its minimum at $2\pi q/M = \pi$ and this is reflected in the l dependence of the correlation function: for l odd, $C(l)$ is negative, whereas for l even, $C(l)$ is positive. The difference between the weak- and strong-coupling values of $C(l)$ decreases with increasing l .

Equation (3.4b) clearly demonstrates that the phenomenon of self-trapping is less clear-cut in case the phonons have a substantial dispersion. The phonon dispersion causes a strong correlation between displacements at different sites and $C(l)$ always shows exponential decay. However, the similarity between dispersionless and dispersive MCM's does not leave any doubt that the same type of transition is taking place.

We have studied the MCM with phonon dispersion in one dimension only. As we showed in I, simulating the dispersionless 3D model is as easy to simulate as the 1D model, but if we extend the 3D model to incorporate phonon dispersion we encounter the problem of evaluating the 4D lattice sum appearing in the expression of $F(l, y)$ [see (3.4e)]. This numerical complication makes the study of the dispersive 3D model much more expensive (from the point of view of computer time) unless we make additional approximations for the phonon spectrum. For instance, we could use a Debye model for the phonons and calculate the integrals analytically. From our experience with the dispersionless MCM and 1D dispersive MCM we do not believe that there will be an essential difference between the 1D, 2D, and 3D models as long as the gap is substantial. In other words, we expect all models to show critical self-trapping effects at nonzero (finite) values of the electron-phonon interaction.

IV. CONCLUSIONS

We have studied the transition between the untrapped and self-trapped states of an electron coupled to a lattice. Starting from Holstein's molecular-crystal model we have constructed a discrete version of the Feynman path integral and showed that it can be used to calculate the electron properties for all values of the electron-phonon interaction. We have demonstrated that for all lattice dimensionalities there exists a critical value of the electron-lattice coupling below which self-trapping does not occur.

For the one- and three-dimensional models our findings disagree with adiabatic studies of the continuum versions of the models. Simulations with model parameters that correspond to the adiabatic regime do not give any evidence that there appear essential differences when one is approaching the adiabatic limit. We conclude that continuum approximations to the MCM, in which there is no inherent upperbound on the kinetic energy of the electron, behave quite differently from Holstein's original discrete lattice model. In addition, we do not find any evidence for coexistence of untrapped and self-trapped polarons in the 3D model.

We have investigated in detail the effect of phonon dispersion in the 1D case and we have presented evidence that the critical value of electron-lattice coupling goes to

zero if the optical phonon becomes soft. A soft optical phonon triggers a lattice-dynamical phase transition and in the context of the MCM it might be considered as somewhat unphysical or, more positively, of academic interest only.

In conclusion, we would like to say that our work has shown that the ground state of the molecular-crystal model, a well-defined "simple" many-body model, is poorly understood. The system behaves quite differently from what could be anticipated from previous, approximate treatments.

ACKNOWLEDGMENTS

We would like to thank J. Fizez for many fruitful discussions and a critical reading of the manuscript. One of us (H.D.R.) thanks the National Fund for Scientific Research (Belgium) for financial support. This work is supported by the Inter-University Institute for Nuclear Sciences (Belgium) and the Dutch Stichting voor Fundamenteel Onderzoek der Materie.

-
- ¹H. De Raedt and A. Lagendijk, *Phys. Rev. Lett.* **49**, 1522 (1982); H. De Raedt and A. Lagendijk, *Phys. Rev. B* **27**, 6097 (1983); the latter will be referred to as I in this paper.
²T. Holstein, *Ann. Phys. (N.Y.)* **8**, 325 (1959); **8**, 343 (1959).
³Y. Toyozawa, *Prog. Theor. Phys.* **26**, 29 (1961); A. Sumi and Y. Toyozawa, *J. Phys. Soc. Jpn.* **35**, 137 (1973).
⁴D. Emin and T. Holstein, *Phys. Rev. Lett.* **36**, 323 (1976).
⁵D. Emin, *Adv. Phys.* **22**, 57 (1973).
⁶J. Appel, in *Solid State Physics*, edited by F. Seitz, D. Turnbull, and H. Ehrenreich (Academic, New York, 1968), Vol. 21.
⁷C. Kittel, *Quantum Theory of Solids* (Wiley, New York, 1963), p. 134.
⁸G. D. Mahan, *Many Particle Physics* (Plenum, New York, 1981).

- ⁹F. S. Ham, in *Electron Paramagnetic Resonance*, edited by S. Geschwind (Plenum, New York, 1972).
¹⁰E. N. Economou, *Green's Functions in Quantum Physics* (Springer, Berlin, 1979).
¹¹P. Prelovšek, *J. Phys. C* **12**, 1855 (1979), and references herein.
¹²H. F. Trotter, *Proc. Am. Math. Soc.* **10**, 545 (1959); M. Suzuki, *Commun. Math. Phys.* **51**, 183 (1976).
¹³R. P. Feynman and A. R. Hibbs, *Quantum Mechanics and Path Integrals* (McGraw-Hill, New York, 1965).
¹⁴S. Golden, *Phys. Rev.* **137**, 1127 (1965); E. Lieb and W. Thirring, *Studies in Mathematical Physics* (Princeton University Press, Princeton, N.J., 1976).
¹⁵K. Binder, *Monte Carlo Methods in Statistical Physics*, edited by K. Binder (Springer, Berlin, 1979).